Surface transfer doping of MoO₃ on hydrogen terminated diamond

with an Al₂O₃ interfacial layer

Yu Yang, 1 Franz A. Koeck, 1 Xingye Wang, 2 and Robert J. Nemanich 1

¹Department of Physics, Arizona State University, Tempe, Arizona 85287-1504, USA

²School for Engineering of Matter, Transport and Energy, Arizona State University, Tempe,
Arizona 85287-6106, USA

Corresponding Author: Robert Nemanich (robert.nemanich@asu.edu)

ABSTRACT

A thin layer of Al₂O₃ was employed as an interfacial layer between surface conductive hydrogen-terminated (H-terminated) diamond and MoO₃ to increase the distance between the hole accumulation layer in diamond and negatively charged states in the acceptor layer, and thus reduce the Coulomb scattering and increase the hole mobility. The valence band offsets are found to be 2.7 and 3.1 eV for Al₂O₃/H-terminated diamond and MoO₃/H-terminated diamond, respectively. Compared to the MoO₃/H-terminated diamond structure, a higher hole mobility was achieved with Al₂O₃ inserted as an interface layer. This work provides a strategy to achieve increased hole mobility of surface conductive diamond by using optimal interlayers with high electron affinity surface acceptor materials.

1

This is the author's peer reviewed, accepted manuscript. However, the online version of record will be different from this version once it has been copyedited and typeset

PLEASE CITE THIS ARTICLE AS DOI: 10.1063/5.0083971

Diamond is a promising candidate for high frequency and high-power electronic devices due to its high thermal conductivity, wide band gap, high carrier mobility and high-saturated drift velocity. Field effect transistors (FETs) based on dielectric layers on hydrogen terminated diamond (H-diamond) show surface conductivity usually ascribed to the formation of a hole accumulation layer [1]. The prior studies, taken together, indicate that charge transfer at the dielectric / Hdiamond interface can lead to a hole accumulation layer but with relatively low mobility attributed to interface scattering from the transferred negative charge [2]. A recent study of FETs from Al₂O₃ / H-diamond has shown high RF performance with an f_T of 30 GHz [1]. A notable aspect of this study is the indication of a carrier velocity of 1×10^7 cm/s, which approaches the saturation velocity of diamond [3]. A second set of papers focused on the low field hole mobility when hexagonal boron nitride (h-BN) is used as the dielectric on H-diamond [4,5,6]. A high channel mobility of ~680 cm²/V-s was achieved [6]. This significant increase of the measured mobility was ascribed to effective reduction of charge scattering at the interface [5,6]. Following the indication of the role of interface scattering, this report presents a different approach to increase the low field channel mobility at the dielectric / H-diamond interface following a strategy similar to modulation doping in III-V heterostructures [7].

While p- and n-type substitutional dopants exhibit high activation energies in diamond, a p-type surface conducting layer can be readily achieved by surface transfer doping at a diamond surface or interface. [1] The conductivity of the surface layer is not thermally activated, which provides an advantage relative to impurity doping in diamond. Indeed, surface transfer doping provides an alternative strategy to enable high power and high frequency diamond field effect transistor (FET) operation. While surface transfer doping was first observed for air exposed H-diamond surfaces, a number of studies have shown surface transfer doping characteristics at dielectric / H-diamond interfaces [8]. The surface conducting layer of both air exposed and dielectric / H-diamond interfaces can reach the following electrical properties: sheet resistance of 5-20 k Ω /sq, hole density of 10^{12} - 10^{13} cm⁻² and hole mobility of 10-150 cm²/V-s [8].

Hydrogen-terminated (H-terminated) diamond (Eg = 5.47 eV) exhibits a negative electron affinity (NEA) of -1.1 \sim -1.3 eV [9]. Consequently, the valence band maximum (VBM) of the H-terminated diamond is \sim 4.3 eV below the vacuum level. Materials with sufficiently high electron affinity (χ > 4.3 eV), such as MoO₃, V₂O₅, WO₃, could align with their conduction band minimum (CBM) below the VBM of H-terminated diamond. Electron transfer, from the diamond to the transition metal oxides, would then be energetically favorable. The relative band alignment of the dielectric layer provides the driving electric potential for the transfer of electron from the diamond valence band to the dielectric layer conduction band or localized defects within the gap [10,11].

While surface conductive diamond may be enabled by high electron affinity metal oxides, a correlation is often observed between hole concentration and mobility where an increase in carrier concentration is associated with a mobility decrease or vice versa [8]. One possibility is that for charge transfer doping, the density of the negatively charged states is not distributed homogenously in the oxide, but accumulate in a layer adjacent to the hole accumulation layer in the diamond [12]. Those negatively charged states give rise to Coulomb scattering in the hole accumulation layer. For bulk-doping of semiconductors, the scattering of free charge carriers at low temperatures is dominated by Coulomb scattering from the ionized impurities. With the Brooks-Herring and Conwell-Weisskopf approximations, the mobility is described by [13]

$$\mu_I = \frac{8\sqrt{2}}{q^3} \left(\frac{k}{\pi}\right)^{\frac{3}{2}} \frac{\varepsilon_r^2 T^{3/2}}{(m^*)^{0.5} N_I f} , (1)$$

where k is the Boltzmann constant, q is the electron elementary charge, ε_r is the relative permittivity, m^* is the effective mass, N_l is the concentration of ionized impurities and f is the screening factor. The Coulomb scattering mechanism results in a carrier mobility that is inversely proportional to the density of charged scattering centers. Similarly, the sheet resistance is described as

$$R_s = 1/\mu q(N_I t) \quad , \quad (2)$$

where t is the layer thickness and $(N_I t)$ is the sheet carrier concentration. For a specific sheet resistance, $\mu q R_s = 1/(N_I t)$ provides the relation of the mobility and sheet charge concentration for a range of values. A larger sheet charge concentration is linearly balanced by a reduction of the mobility.

For charge transfer doping, the results from temperature-dependent Hall effect measurements also confirm this [12]. As the density of negatively charged states in the adsorbate or dielectric layer is approximately equal to the hole sheet concentration in the diamond, an increase in the hole sheet concentration is associated with an increase of negatively charged states in the adsorbate or dielectric layer. Furthermore, the increased density of negatively charge states would result in a reduction of hole mobility due to the Coulomb scattering.

On the other hand, the potential of a charged scattering center v(r) is $\sim 1/|r|$. When the negatively charged states accumulate adjacent to the hole accumulation layer, the effect of Coulomb scattering is significant and limits the hole mobility [2,4]. This effect has also been analyzed in detail for modulation doping in AlGaAs/GaAs heterostructures. Here, impurity doping in the AlGaAs layer can provide electrons to the GaAs charge accumulation layer which reduces the ionized impurity scattering and the mobility is projected to increase as $d^{5/2}$ where d is the location of the dopants relative to the interface [7]. Following the example of modulation doping in AlGaAs/GaAs, we propose to employ a thin layer of Al₂O₃ as an interfacial layer between diamond and MoO₃ to increase the distance between the hole accumulation layer in diamond and the negatively charged states in the acceptor layer.

This study presents photoemission measurements of the electronic band alignment of the MoO_3 / Al_2O_3 / H-diamond layer structure to gain insight into the driving potential for the negative charge transfer and the location of the negative charges near the interface, in the Al_2O_3 layer or in the MoO_3 layer.

The diamond substrates used in this study were $5 \times 5 \text{ mm}^2$ type IIa chemical vapor deposited

4

single crystalline undoped diamond (100) substrates. A hydrogen plasma treatment was applied for 15 min to obtain an H-terminated surface. Hydrogen terminated surfaces were prepared in a microwave plasma chemical vapor deposition system used for diamond layer growth. The process was applied for 15 min using a microwave power of 1000 W and $\rm H_2$ pressure of 50 Torr. The diamond substrate reached ~800 °C due to heating from the plasma.

The Al₂O₃ deposition was accomplished by remote plasma enhanced atomic layer epitaxy (PEALD). The precursor used was dimethylaluminum isoproxide (DMAI, [(CH₃)₂AlOCH(CH₃)₂]₂) and an O₂ plasma was used as the oxidizer [14]. The oxygen plasma was excited with 30 W rf power. The growth rate was ~1.5 Å/cycle at a substrate temperature of 100 °C.

After Al_2O_3 deposition, the surface was processed with a hydrogen plasma post-deposition treatment for 30 min at ~500 °C. The hydrogen plasma was excited by 100W rf power. The chamber pressure was maintained at 100 mTorr with a constant H_2 gas flow of 20 sccm. Additional details are presented in our previous work [14].

Molybdenum oxide layers were deposited in a reactive electron beam deposition (EBD) system, which has a base pressure of 1×10^{-8} Torr. Molybdenum pellets with a purity of 99.99% were evaporated using an e-beam. After deposition the substrates were transferred (in UHV) to the PEALD system where an O-plasma process was employed. The MoO₃ (+6) oxidation state was achieved using a 5 min oxygen plasma treatment at ambient temperature. The remote plasma was generated by 30 W rf excitation with a 100 mTorr oxygen pressure. The oxidation state of the molybdenum oxide layers was examined with XPS.

The hole accumulation layer is associated with upward band bending in the diamond near surface region. Consequently, the surface conducting state can be indicated by measuring the binding energy of the C 1s core level. After each process (Al₂O₃ deposition, hydrogen plasma, Mo deposition, oxygen plasma), the surface was characterized using *in situ* XPS, which employed a monochromated Al K_{α} X-ray source (hv = 1486.6 eV) with a bandwidth of 0.2 eV and a R3000

Scienta analyzer with a resolution of 0.1 eV. All core level spectra were recorded with a 0.05 eV step, and the peak positions can be resolved to $\sim \pm 0.05$ eV by curve fitting.

Ex-situ Hall effect measurements were performed using an Ecopia HMS-3000 Hall measurement system. The diamond was mounted on a Van der Pauw-Hall probe. A \sim 0.5 mm diameter dot of gold foil was used under each probe tip to increase the contact area. The surface resistance, carrier density, and carrier mobility were measured with a 0.51 T permanent magnet at room temperature.

Diamond samples using MoO₃ as acceptor layer were prepared with 0, 2 nm, and 4 nm Al₂O₃ interface layers. For the H-terminated diamond surface with air exposure, the C 1s core level was located at a characteristic position 284.1 eV, indicating the surface conductive state [14]. After 2 nm MoO₃ deposition by EBD, the spectrum of the Mo 3d_{3/2} and 3d_{5/2} spectral region shows three peaks which is a superposition from metallic Mo regions and partially oxidized Mo regions (Fig. 1c). The peak near 228 eV corresponds to the 3d_{5/2} core level of metallic Mo regions, the central peak is a combination of the 3d_{3/2} from the metallic regions and the 3d_{5/2} of partially oxidized Mo. The third peak at ~235 eV is the 3d_{3/2} of the partially oxidized Mo. After the oxygen plasma process, the molybdenum is fully oxidized, and the remining two peaks correspond to the Mo 3d_{3/2} and 3d_{5/2} core levels shifted to higher binding energies of 235.7 eV and 232.5 eV. These values indicate Mo in the +6 oxidation state (for MoO₃) in Fig 1 as well as the samples described in Fig 2 and Fig. 3. The C 1s core level was not affected by the MoO₃ deposition. Fig. 1 shows the C 1s, O 1s, and Mo 3d core levels of the diamond surface after each process.

For the diamond samples that employed 2 nm Al₂O₃ interfacial layers, the C 1s core level shifted to higher binding energy after Al₂O₃ PEALD, as shown in Fig. 2. With a hydrogen plasma post-deposition treatment, the C 1s core level was restored to 284.0 eV, the characteristic binding energy of the surface conducting state, consistent with our previous study [14]. The Al 2p core level shifted 2.1 eV to a higher binding energy 75.3 eV, indicating that the hydrogen plasma

process not only restored the hole accumulation layer in diamond, but also resulted in a negatively charged layer at the interface. The negatively charged interfacial layer, which was adjacent to the diamond hole accumulation layer, would introduce the Coulomb scattering of the holes, limiting the hole mobility. After MoO₃ deposition, the Al 2p core levels shifted 0.9 eV to lower binding energy, indicating a reduced density of negative charges close to diamond surface. Apparently, the Coulomb scattering due to the negatively charged interfacial layer was reduced. The C 1s core level position of the diamond was not affected by the MoO₃ deposition, confirming the diamond surface remained in the conductive state.

For the diamond samples with 4 nm Al₂O₃ interfacial layer, after hydrogen plasma treatment, the C 1s core level at 284.2 eV (as shown in Fig. 3) was not fully restored (to 284.0 eV) characteristic of the surface conducting layer. The result may indicate that the hydrogen plasma is less effective restoring the surface conductivity for the thicker Al₂O₃ layers. However, with the addition of 2 nm of MoO₃ the C 1s core level shifted from 284.2 eV to 284.0 eV, indicating electron transfer from the diamond to the MoO₃ acceptor layer.

Table 1 summarizes the change of sheet resistance, hole concentration and hole mobility of H-terminated diamond with MoO₃ as acceptor layer and Al₂O₃ as an interface layer. The air exposed, hydrogen terminated surfaces exhibit sheet resistance consistent with many other reports [1]. The properties of the surface such as roughness and hydrogen termination contribute to the charge density and mobility of the specific surfaces [15]. For the sample without Al₂O₃, the surface conductivity of diamond was achieved with MoO₃ as an acceptor layer. After MoO₃ deposition and oxidation, the sheet resistance increased to 6.9 kΩ/sq, and remained under 10 kΩ/sq. The hole concentration remained the same as the H-terminated surface while the hole mobility decreased to 8.9 cm²/(Vs). For the samples with an Al₂O₃ interface layer, the surface conductivity was achieved with the diamond/Al₂O₃/MoO₃ structure. The sheet resistance increased similarly as without Al₂O₃ to 5.9 kΩ/sq and 14.0 kΩ/sq, and the hole concentration decreased to 9.4×10¹²/cm² and

 3.5×10^{12} /cm², for the samples with 2 nm and 4 nm Al₂O₃, respectively. The hole mobility increased significantly to >100 cm²/V-s. The change of sheet resistance, hole concentration and hole mobility for the different structures with processes are plotted in Fig. 4(a), and the hole concentration and mobility of different structures are compared in Fig. 4(b). The hole mobility and concentration vary with the change of the thickness of Al₂O₃.

The valence band offset (ΔEv) between diamond and Al_2O_3 can be calculated using the following equation [16,17]:

$$\Delta E_{V} = (E_{CL} - E_{V})_{Diamond} - (E_{CL} - E_{V})_{Al_{2}O_{3}} - \Delta E_{CL}$$
, (3)

where E_{CL} is the binding energy of the XPS core level; E_{V} is the valence band maximum (VBM); (E_{CL} - E_{V}) is the binding energy difference from the VBM to the respective core level; and ΔE_{CL} is the binding energy difference between the diamond and $Al_{2}O_{3}$ core levels measured at the interface ($E_{CL}^{C_{18}}$ - $E_{CL}^{Al_{2p}}$). The value of (E_{CL} - E_{V}) $Al_{2O_{3}}$ was 70.6 ± 0.1 eV [18] and (E_{CL} - E_{V})Diamond was 284.1 ± 0.1 eV. The diamond value was based on the assumption that the VBM is at the Fermi level for the surface conductive state. The VBO between $Al_{2}O_{3}$ and diamond was determined to be 2.6 eV by using Eq. (3), and taking account a band bending of 1.2 eV, which resulted from a concentration of defects or interstitial oxygen atoms in $Al_{2}O_{3}$ introduced by oxygen plasma [14]. The ΔE_{V} between diamond and MoO_{3} was calculated to be 3.1 eV by using Eq. (3), where (E_{CL} - E_{V}) MoO_{3} was 229.5 eV as the Fermi level of MoO_{3} is located close to its conduction band minimum (CBM).

The band diagrams of Al₂O₃ / H-diamond, and MoO₃ / Al₂O₃ / H-diamond are shown in Fig. 5. The charge at the Al₂O₃ / H-diamond interface is represented by a decrease of the band displacement. After MoO₃ was deposited on Al₂O₃, the Al 2p core level shifted to lower binding energy. This result indicated that the distribution of negative charges changed and part of the negative charges originally close to diamond interface transferred into the MoO₃ layer.

According to the position of the Al 2p core level, the distribution of negative charge changes

level difference between the diamond VBM and the acceptor level, the sheet concentration and mobility of the hole accumulation layer are related to the oxide electron affinity. A higher electron affinity of the acceptor material corresponds to a larger energy difference with the diamond valence band. Evidently, oxides with a higher electron affinity lead to a higher sheet hole concentration and a lower hole mobility. Without the Al₂O₃ interfacial layer, the sheet concentration and mobility of the hole accumulation layer achieved with MoO₃, are mainly determined by its electron affinity. With a thin Al₂O₃ interfacial layer, the MoO₃ acts as an additional acceptor layer, where a fraction of the negative charges are located at the Al₂O₃ / H-diamond interface and the other negative charges are distributed in the MoO₃. When the Al₂O₃ is sufficiently thick the negatively charged interfacial layer limits the hole mobility by Coulomb scattering.

with the increase of the Al₂O₃ layer thickness. As the charge transfer doping is driven by the energy

We note that reducing the negative charge in the Al₂O₃ could substantially improve the efficiency of charge transfer away from the interface. Our previous study explored a 500 °C anneal after the Al₂O₃ ALD deposition and H-plasma process, but a reduction in the interface charge was not detected [14]. Other approaches for Al₂O₃ deposition, such as high temperature ALD, could potentially improve the process [19]. We also note that effects related to interface roughness, defects and impurities could play a significant role in the charge transfer process [20].

For an Al₂O₃ interlayer, as the thickness increases from 0 to 4 nm, the hole concentration decreases and the mobility increases. This effect could be quantified with Hall measurements which are planned for the future. The hole concentration decrease is because the distance between the diamond and acceptor layer increases, while the potential difference between the diamond and oxide bands (i.e. band offset) is unchanged. If the charge distribution is simplified to all holes accumulated at the interface of Al₂O₃ / H-diamond and all negative charged states accumulated at the interface of Al₂O₃ / MoO₃, the hole concentration in diamond can be estimated by comparison to the ideal capacitor relations: $Q = CV = (\epsilon A/d) V$, where C is the capacitance, ϵ is the dielectric

constant, A is the contact area, d is the Al_2O_3 thickness, and V is the (before equilibrium) energy difference between the H-diamond VBM and the MoO_3 conduction band. In this case, an increase of Al_2O_3 thickness results in a decrease of hole concentration. Although in the MoO_3 / Al_2O_3 / H-diamond structure, the negatively charged states distribute at both the Al_2O_3 / H-diamond interface and the MoO_3 / Al_2O_3 interface. The increase of the distance between H-diamond and MoO_3 results in a decrease of the charge transfer between H-diamond and MoO_3 .

Insight into the charge distribution can be established with capacitance-voltage measurements as has been demonstrated in recent studies of dielectric layers on H-terminated diamond [21,22]. Such studies are being considered for future studies of dielectric layers on H-diamond.

The increase of the hole mobility may be attributed to the reduced Coulomb scattering with the increase of the distance between the hole accumulation layer and the negative charged states. At a certain point the increase of the Al₂O₃ layer thickness limits the charge transfer to the MoO₃ structure, and the interface turns into the case of thick Al₂O₃ on H-diamond [14].

In this work, a surface conducting layer was achieved using MoO₃ as a charge transfer layer with a thin Al₂O₃ interfacial layer. The VBO are found to be 2.6 eV and 3.1 eV for Al₂O₃ / H-terminated diamond and MoO₃ / H-diamond, respectively. The band alignment provides the driving potential for charge transfer. The diamond sheet resistance, hole concentration and mobility were characterized for MoO₃ / H-diamond with Al₂O₃ interfacial layers of 0, 2, and 4 nm thickness. By combining two oxides (Al₂O₃ and MoO₃), the hole mobility and concentration were modulated by altering the thickness of the interfacial layer. The mobility of the hole accumulation layer on diamond was improved by inserting an interfacial layer to reduce interface scattering. The overall sheet resistance for the different Al₂O₃ interlayers remained constant, which suggests that the charge at the Al₂O₃ / H-diamond interface still limited the mobility. Improvement of the diamond Al₂O₃ / H-diamond interface guided by structural and chemical analysis and Hall measurements could substantially impact the interface mobility. The results also motivate further study of

AP

This is the author's peer reviewed, accepted manuscript. However, the online version of record will be different from this version once it has been copyedited and typeset. PLEASE CITE THIS ARTICLE AS DOI: 10.1063/5.0083971

alternative dielectric materials, with lower defect density, to serve as interlayers between the charge transfer dielectric and H-diamond.

This research was supported by a grant from MIT -Lincoln Laboratories and the NSF through grants DMR -1710551 and DMR -2003567.

AUTHOR DECLARATIONS

Conflict of Interest

The authors have no conflicts to disclose.

DATA AVAILABILITY

The data that support the findings of this study are available from the corresponding author upon reasonable request

This is the author's peer reviewed, accepted manuscript. However, the online version of record will be different from this version once it has been copyedited and typeset

PLEASE CITE THIS ARTICLE AS DOI: 10.1063/5.0083971

REFERENCES

- [1] K.G. Crawford, I. Maini, D.A. Macdonald, D.A.J. Moran, "Surface transfer doping of diamond: A review," Prog. Surf. Sci. 96, 100613 (2021).
- [2] G. Daligou and J. Pernot, "2D hole gas mobility at diamond/insulator interface," Appl. Phys. Lett. 116, 162105 (2020).
- [3] S. Imanishi, K. Horikawa, N. Oi, S. Okubo, T. Kageura, A. Hiraiwa, and H. Kawarada, "3.8 W/mm RF Power Density for ALD Al₂O₃-Based Two-Dimensional Hole Gas Diamond MOSFET Operating at Saturation Velocity," IEEE Elect. Dev. Lett. 40, 279 (2019).
- [4] Y. Sasama, T. Kageura, K. Komatsu, S. Moriyama, J. Inoue, M. Imura, K. Watanabe, T. Taniguchi, T. Uchihashi, and Y. Takahide, "Charge-carrier mobility in hydrogen-terminated diamond field-effect transistors," Journal of Applied Physics 127, 185707 (2020).
- [5] Y. Sasama, K. Komatsu, S. Moriyama, M. Imura, T. Teraji, K. Watanabe, T. Taniguchi, T. Uchihashi, and Y. Takahide, "High-mobility diamond field effect transistor with monocrystalline h-BN gate dielectric," APL Materials 6, 111105 (2018).
- [6] Y. Sasama, T. Kageura, M. Imura, K. Watanabe, T. Taniguchi, T. Uchihashi, and Y. Takahide, "High-mobility p-channel wide-bandgap transistors based on hydrogen-terminated diamond/hexagonal boron nitride heterostructures," Nature Electronics 5, 37-44 (2022). https://doi.org/10.1038/s41928-021-00689-4
- [7] K. Lee, M.S. Shur, T.J. Drummond, and H. Morkoc, "Low field mobility of 2-d electron gas in modulation doped Al_xGa_{1-x}As/GaAs layers," J. Appl. Phys. 54, 6432 (1983).
- [8] C. Verona, W. Ciccognani, S. Colangeli, E. Limiti, M. Marinelli, and G. Verona-Rinati, "Comparative investigation of surface transfer doping of hydrogen terminated diamond by high 12

electron affinity insulators," Journal of Applied Physics 120, 025104 (2016).

[9] D. Takeuchi, H. Kato, G. S. Ri, T. Yamada, P. R. Vinod, D. Hwang, C. E. Nebel, H. Okushi, and S. Yamasaki, "Direct observation of negative electron affinity in hydrogen-terminated diamond surfaces," Applied Physics Letters **86**, 152103 (2005).

[10] S.A.O. Russell, L. Cao, D. Qi, A. Tallaire, K.G. Crawford, A.T.S. Wee, and D.A.J. Moran, "Surface transfer doping of diamond by MoO₃: A combined spectroscopic and Hall measurement study," Applied Physics Letters **103**, 202112 (2013).

[11] K.G. Crawford, L. Cao, D. Qi, A. Tallaire, E. Limiti, C. Verona, A.T.S. Wee, and D.A.J. Moran, "Enhanced surface transfer doping of diamond by V₂O₅ with improved thermal stability," Applied Physics Letters **108**, 42103 (2016).

[12] C.E. Nebel, "Surface transfer-doping of H-terminated diamond with adsorbates," New Diamond and Frontier Carbon Technology **15**, 247 (2005).

[13] K. Somogyi, "Classical approximations for ionised impurity scattering applied to diamond monocrystals," Diamond and Related Materials 11, 686 (2002).

[14] Y. Yang, F.A. Koeck, M. Dutta, X. Wang, S. Chowdhury, and R.J. Nemanich, "Al₂O₃ dielectric layers on H-terminated diamond: Controlling surface conductivity," Journal of Applied Physics **122**, 155304 (2017).

[15] T. Wade, M.W. Geis, T.H. Fedynyshyn, S.A. Vitale, J.O. Varghese, D.M. Lennon, T.A. Grotjohn, R.J. Nemanich, M.A Hollis "Effect of surface roughness and H-termination chemistry on diamond's semiconducting surface conductance," Diamond and Related Materials 76, 79 (2017).

[17] E.A. Kraut, R.W. Grant, J.R. Waldrop, and S.P. Kowalczyk, "Interface contributions to heterojunction band discontinuities: X-ray photoemission spectroscopy investigations," in Heterojunction Band Discontinuities: Physics and Device Applications, edited by F. Capasso and G. Margaritondo (Elsevier, New York, 1987).

[18] J. Yang, B.S. Eller, M. Kaur, and R.J. Nemanich, "Characterization of plasma-enhanced atomic layer deposition of Al2O3 using dimethylaluminum isopropoxide," Journal of Vacuum Science & Technology A 32, 21514 (2014).

[19] A. Daicho, T. Saito, S. Kurihara, A. Hiraiwa and H. Kawarada, "High-reliability passivation of hydrogen-terminated diamond surface by atomic layer deposition of Al2O3," J. Appl. Phys. 115, 223711 (2014).

[20] D. Oing, M. Geller, A. Lorke, and N. Wöhrl, "Tunable carrier density and high mobility of two-dimensional hole gases on diamond: The role of oxygen adsorption and surface roughness," Diamond & Related Materials 97, 107450 (2019).

[21] P. B. Shah, J. Weil, A. G. Birdwell, and T. Ivanov, "Charge trapping analysis of high speed diamond FETs," MRS Advances 2, 2235 (2017).

[22] N. C. Saha and M. Kasu, "Heterointerface properties of diamond MOS structures studied using capacitance-voltage and conductance-frequency measurements," Diamond and Related Materials 91, 219 (2019).



This is the author's peer reviewed, accepted manuscript. However, the online version of record will be different from this version once it has been copyedited and typeset.

TABLE 1 Hall measurement sheet resistance, carrier concentration and carrier mobility of diamond surfaces using MoO₃ as acceptor layer with 0, 2, and 4 nm Al₂O₃ interfacial layers.

Sample	Process	Sheet Resistance (kΩ/sq)	Carrier Concentration /cm ²	Carrier Mobility cm ² /V-s
0 nm Al ₂ O ₃ interfacial layer	H-terminated surface	1.8	1.9×10^{14}	18.4
	After molybdenum dep.	3.6	1.3×10^{14}	13.5
	Oxidation by plasma	6.9	1.0×10^{14}	8.9
2 nm Al ₂ O ₃ interfacial layer	H-terminated surface	2.3	7.0×10^{14}	3.94
	2 nm Al ₂ O ₃ dep. & Hydrogen plasma	2.0	6.4×10 ¹⁴	4.94
	Molybdenum dep. & Oxidation by plasma	6.2	9.4×10^{12}	100.7
4 nm Al ₂ O ₃ interfacial layer	H-terminated surface	5.9	4.6×10^{13}	22.9
	4 nm Al ₂ O ₃ dep. & Hydrogen plasma	11.5	6.7×10 ¹³	8.1
	Molybdenum dep. & Oxidation by plasma	14.0	3.5×10^{12}	125.9

Figure Captions:

Figure 1. XPS scans of MoO $_3$ / H-diamond after each process, showing the (a) O 1s, (b) C 1s, and (c) Mo 3d core level peaks. The results indicate MoO $_3$ after the oxygen plasma.

Figure 2. XPS scans of MoO₃ / 2 nm Al₂O₃ / H-diamond after each process step, showing the (a) O 1s, (b) C 1s, (c) Mo 3d, and (d) Al 2p core level peaks. The results indicate MoO₃ and diamond surface conductivity after the O-plasma.

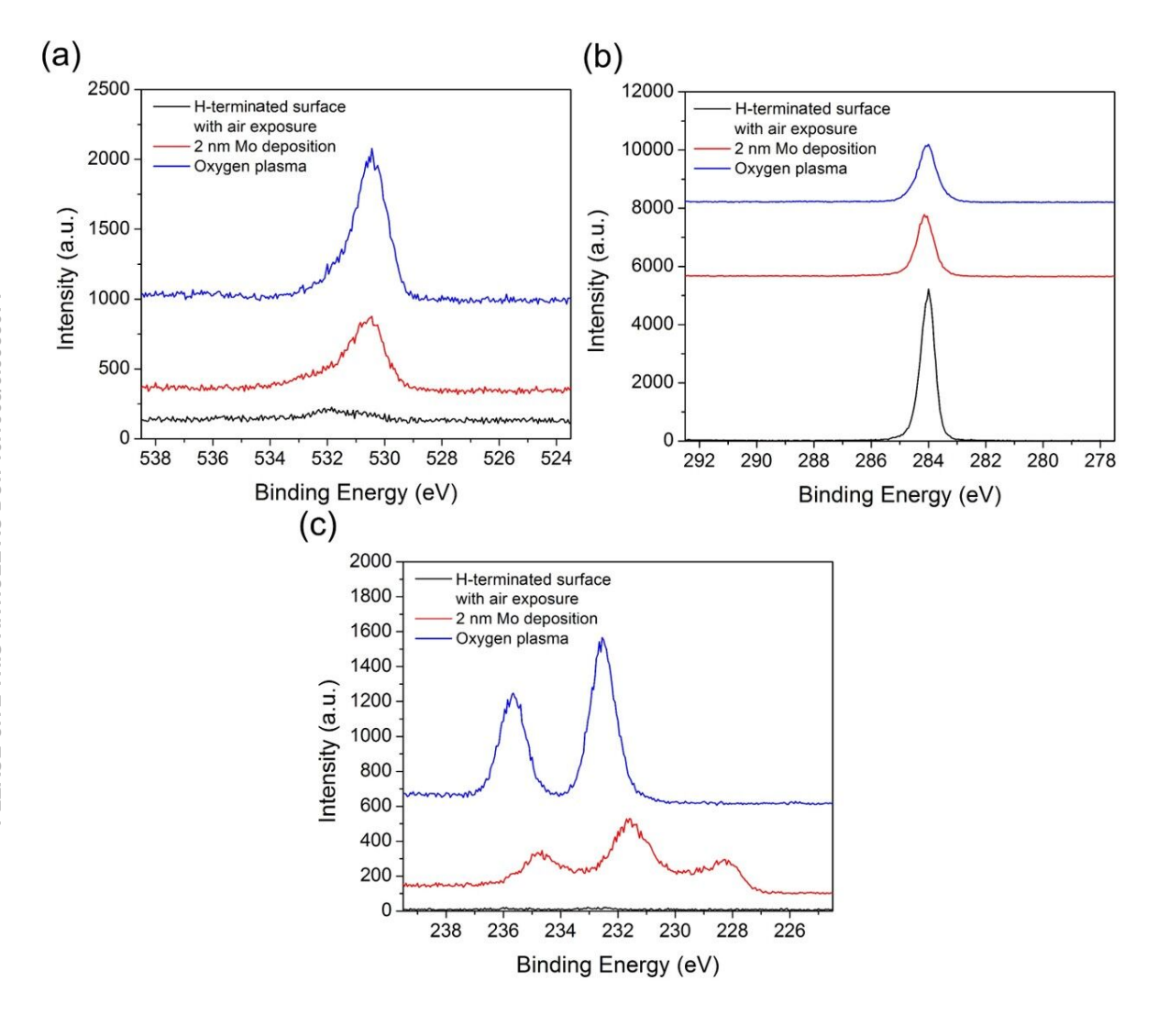
Figure 3 XPS scans of MoO₃ / 4 nm Al₂O₃ / H-diamond after each process step, showing the (a) O 1s, (b) C 1s, (c) Mo 3d, and (d) Al 2p core level peaks. The results indicate MoO₃ and diamond surface conductivity after the O-plasma.

Figure 4 (a) The change of sheet resistance, hole concentration and hole mobility with processes for MoO_3 / 0/2/4 nm Al_2O_3 / H-diamond. (b) The hole concentration and mobility of different structures. The lines indicate constant sheet resistance.

Fig. 5. Band diagrams of MoO $_3$ / H-diamond, Al $_2$ O $_3$ / H-diamond and MoO $_3$ / Al $_2$ O $_3$ / H-diamond. Excess charges are indicated as well as the hole accumulation layer near the diamond interface.

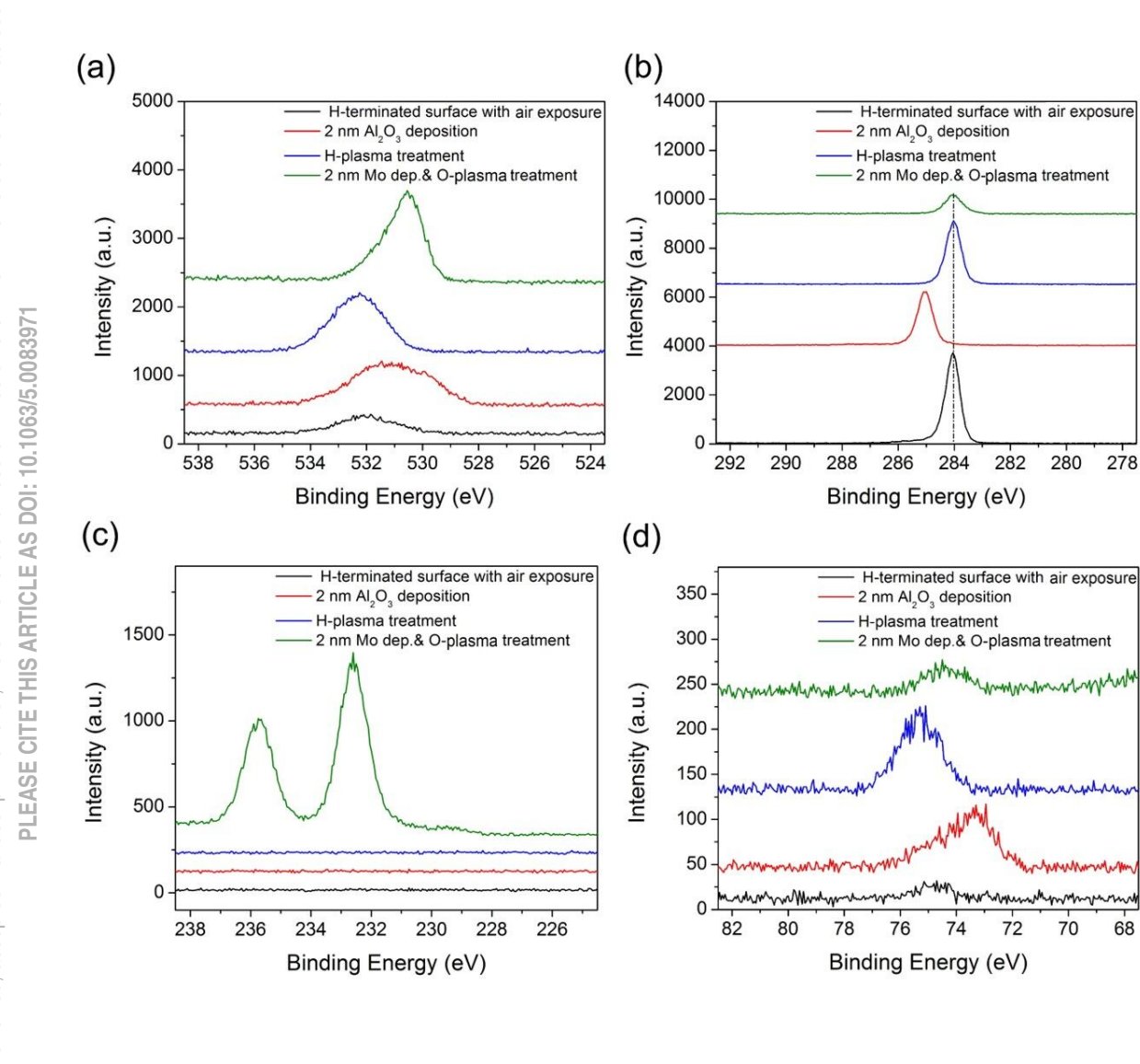


This is the author's peer reviewed, accepted manuscript. However, the online version of record will be different from this version once it has been copyedited and typeset.





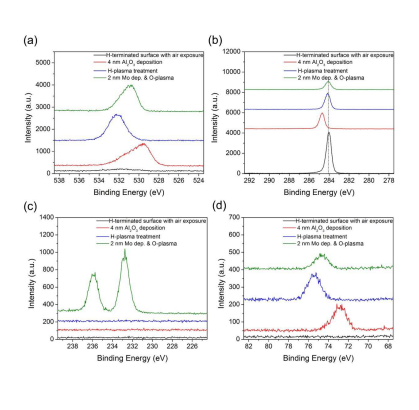
This is the author's peer reviewed, accepted manuscript. However, the online version of record will be different from this version once it has been copyedited and typeset.





ACCEPTED MANUSCRIPT

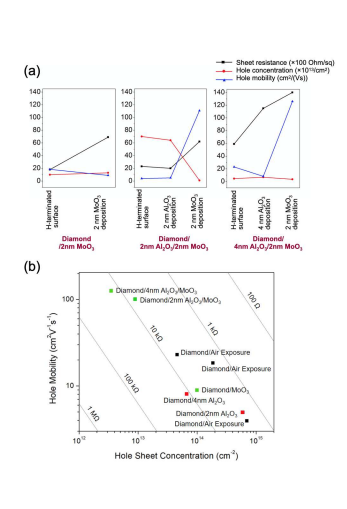
This is the author's peer reviewed, accepted manuscript. However, the online version of record will be different from this version once it has been copyedited and typeset.





ACCEPTED MANUSCRIPT

This is the author's peer reviewed, accepted manuscript. However, the online version of record will be different from this version once it has been copyedited and typeset.





ACCEPTED MANUSCRIPT

This is the author's peer reviewed, accepted manuscript. However, the online version of record will be different from this version once it has been copyedited and typeset.

